A multi-scale hybrid approach to the modelling and design of a novel micro-channel cooling structure for the W7X divertor

Case Studies in Thermal Engineering 42 (2023) 102734

Contents lists available at ScienceDirect

Case Studies in Thermal Engineering

journal homepage: www.elsevier.com/locate/csite

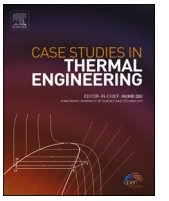

A multi-scale hybrid approach to the modelling and design of a novel micro-channel cooling structure for the W7X divertor

Hossein Ebadi [a], Francesco Carrone [a,b], Rosa Difonzo [a], Joris Fellinger [b], Heinrich P. Laqua [b], Niko Schneider [b], Laura Savoldi [a,*]

[a] MAHTEP Group, Dipartimento Energia "Galileo Ferraris", Politecnico di Torino, Torino, Italy
[b] Max-Planck-Institute for Plasma Physics, Greifswald, Germany

ARTICLE INFO

Keywords:
Additive manufacturing
Micro-channels
Cooling
Modelling
Porous medium
Divertor

ABSTRACT

The second operating phase of the W7X stellarator, with an expanded set of plasma-facing components, includes the test of divertor tiles with a continuous heat load reaching 10 MW/m^2. The divertor tiles are cooled by subcooled water. Here a novel cooling concept, based on a network of parallel arrays of micro-channels (MC) with sub-millimetre dimensions, is investigated on a 0.1 m × 0.1 m tile, realizable by Additive Manufacturing. Detailed CFD simulations of the mock-up are performed to check the cooling uniformity using a multi-scale approach, aiming at limiting the dimension of the computational grid without a major loss of accuracy. First, the detailed hydraulic and thermal characterization on a sub-domain with of a small group of MC is performed. Then, the block of MC is substituted with an equivalent porous strip (PS), calibrating the hydraulic and thermal characteristics of the porous medium. The model is verified on an array of MCs or PSs connected to the same manifolds, showing the capability to reproduce the pressure drop and temperature increase with maximum errors of 1.05% and ∽20% in nominal conditions, respectively. The numerical model of the entire tile equipped with PSs is then reliably adopted to evaluate the thermal-hydraulic performance of the cooling device.

1. Introduction

One of the promising options which could contribute to the decarbonization of the power sector in the second half of the century is nuclear fusion [1,2]. Notwithstanding the main research stream focused on tokamak configuration, the magnetic-confinement stellarator option [3] is also under investigation and few remarkable experiments are running in EU (the Weldenstein7-X [4]) and Japan (the Large Helical device, LHD [5]).

After the successful operation [6], the W7X stellarator [3] is under refurbishment towards a second operating phase, with an expanded set of plasma-facing components compared to the first phase [7]. Among the others, the test of divertor tiles is included, with a continuous heat load that can reach 10 MW/m^2 and cooling provided by subcooled water at 20–30 °C, pressurized at 2.4 MPa. Beside the traditional cooling solutions [8], such as, among others, hypervapotrons [9], rectangular heat sinks [10] and channels with twisted tapes [11], several cooling options could be of interest, also thanks to the development of Additive Manufacturing techniques. Here a novel cooling concept, based on a network of parallel arrays of rectangular channels, with sub-millimetre dimensions (micro-channels, MC) and connected by Z-manifolds, is investigated. This concept, very well known in other applications such as miniaturized electronic

* Corresponding author.
E-mail address: laura.savoldi@polito.it (L. Savoldi).

https://doi.org/10.1016/j.csite.2023.102734
Received 16 October 2022; Received in revised form 19 December 2022; Accepted 14 January 2023
Available online 19 January 2023

devices [12], was originally designed for cylindrical cavity cooling in high power gyrotron [13], but was adapted to planar geometry. A 0.1 m × 0.1 m flat tile has been designed with such cooling option, see Fig. 1, to be tested in the GLADIS facility at IPP [14], under intense ion beams flux and cooled by 50 l/min of subcooled water at 27 °C and 0.75 MPa. The tile is made of copper with a tungsten layer on top of it, receiving the heat load. Notwithstanding the tapering of the water manifolds, already included to achieve some level of homogeneity of the flow through the MCs along the manifold [15,16], see Fig. 1, detailed Computational Fluid Dynamic (CFD) simulations of the mock-up are needed in order to check the uniformity of the cooling capability underneath the heated surface already in the design phase. However, solving the standard conjugate heat transfer problem in the MC necessitates a significant numerical effort, because of the very large computational grid required to model the >1500 MCs inserted in the structure.

Here we develop for the thermal-hydraulic analysis of the tile a multi-scale approach, aiming at limiting the dimension of the computational problem. The approach is based on the introduction of an equivalent porous medium, to substitute groups of MC, similarly to the strategy already adopted for the hydraulic analysis of other cooling components requiring a large computational effort such as the detailed analysis of the distributing manifolds for the EU-DEMO Water-Cooled Lithium–Lead blanket [17]. First, the detailed hydraulic and thermal characterization of a sub-domain containing a group of 6 MCs in parallel is performed within a wide range of mass flow rates spanning from laminar to turbulent regime. Then, the block of 6 parallel MCs is substituted with an equivalent porous strip (PS), suitably calibrating the porous medium viscous and inertia coefficients in the Darcy-Forchheimer formulation, to obtain a comparable hydraulic characteristic in the PS. A similar procedure is followed for the thermal characterization of the PS, calibrating its effective conductivity. While the calibration of the PS is performed on a subset of 6 MCs in parallel, the validation of the equivalent model is performed on a more extended computational domain, considering the entire length of an inlet/outlet manifold (called here “array”), following a multi-scale approach. Once the model of an entire array equipped with PSs is successfully compared against the array equipped with MCs and its error assessed, the equivalent models with all the MCs substituted with PSs can be used to assess the homogeneity in the flow repartition and the cooling capability of the entire tile, with a significant reduction of the computational effort.

The approach is hybrid, in the sense that the manifolds for the coolant are modeled as clear channels by means of standard single-phase CFD models, while the MCs connecting the manifolds are substituted by porous strips in parallel. Note that the methodology already developed in Ref. [17] for the hydraulic characterization has been extended here also to include the thermal characterization of the equivalent porous medium.

2. Development and calibration of an equivalent porous strip

An equivalent porous strip is developed here to mimic the hydraulic and thermal behavior of 6 MCs connected in parallel to the same inlet and outlet manifold. The number of MCs to be used as the basis for the development of the PS has been selected as a first tradeoff between two aspects. The first is the targeted reduction in the computational effort, that pushes to include the highest possible number of MCs in the PS. The second is the need to preserve a representative distribution of flow repartition along the length of the manifolds, that pushes in the opposite direction.

Since the hybrid approach is adopted here attempting to explore a wide range of Reynolds numbers, attention is put on the selection of the most suitable model for the fluid, to return accurate results in a range of coolant flow as wide as possible. When a liquid working fluid is running through the micro-channels, laminar-to-turbulent flow transition turbulence models are advised [18] for a better understanding of mixing and heat transfer in microsystems. Accordingly, in the simulation setup (Fig. 2c), the $\kappa-\omega$ SST transition model has been selected as a turbulence closure since it guarantees reliable results from the fully turbulent regime down to the laminar one, passing through the transition region. The γ-transition model was chosen, which is advantageous when the estimation of boundary layer edges is difficult and there is no prior assumption about the flow field.

To confirm the suitability of the selected turbulence model for the MC simulation, a comparison with the more advanced Reynolds Stress Model, and a more detailed analysis performed by unsteady Large Eddy Simulations in a single MC were performed. They both returned the same pressure drop computed with the $\kappa-\omega$ SST γ-transition model with an accuracy within few percent. Note that in the

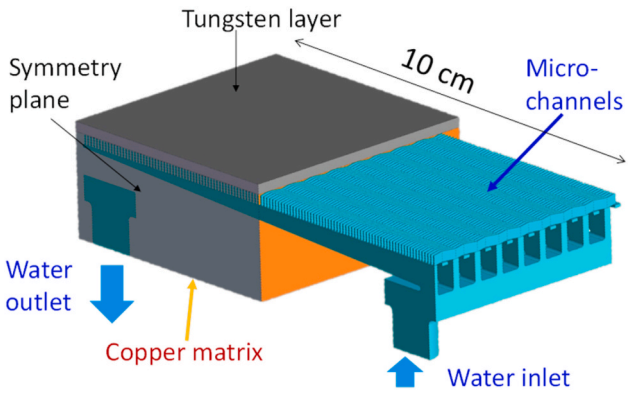

Fig. 1. Schematic view of the MCs cooling structure of half divertor tile.

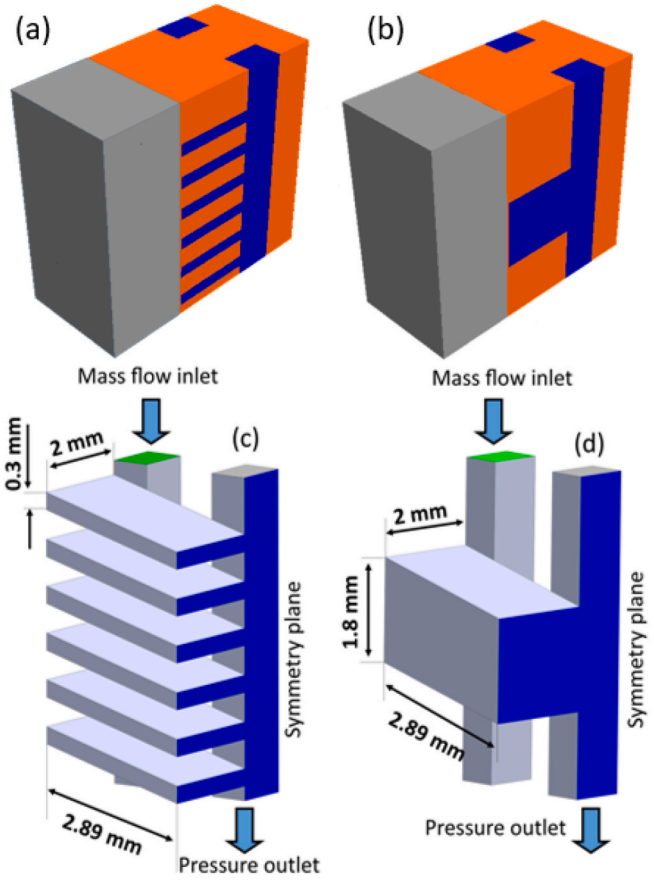

Fig. 2. Geometry of a portion of a tile with the block of 6 MCs connected in parallel (a) and of the equivalent PS (b), with the corresponding cooling path (c, d), respectively.

hybrid simulations no turbulence is modeled within the PS, so that the fluid does not carry any turbulent kinetic energy nor specific rate of dissipation when it exits the PS and enters the outlet manifolds. This constitutes an intrinsic difference between the MC and the PS models, that we estimate to be small.

The computational grid developed in the MC region can thus account for significant velocity gradients at the wall through 6 layers of prismatic cells which can be avoided in the porous medium. Details of the grid independence study are summarized in Table 1, considering 6 different meshes and the relative pressure drop ratios to the reference (finest) mesh. The average cell size in the table was computed as $\sqrt[3]{V/N_{cell}}$, where V is the total volume of the mockup, and N_{cell} is the cell number. The grid adopted for the simulations is #5, which shows a numerical accuracy of 0.2% if compared to the finest one. The total number of elements for the computational domain shown in Fig. 2c is 1 Mcells, while for the PS in Fig. 2d is 0.1 MCells.

The SIMPLE algorithm for the steady-state simulation with incompressible water as coolant is selected, with a segregated solver, using the STAR-CCM + commercial software [19]. The segregated energy approach is used adding the thermal model to the hydraulic one in the conjugate heat transfer analysis.

2.1. Hydraulic characteristic

The pressure drop across the sub-size configuration of the 6 MCs in parallel (Fig. 2c) is computed for a mass flow rate spanning from

Table 1
Results of the grid independence analysis on the computed pressure drop across the sub-size configuration of 6 MC in parallel.

Mesh No.	Average cell size (mm) $\times 10^{-5}$	$\Delta P/\Delta P_{ref}$
1	1.43	0.949
2	0.74	0.971
3	0.45	0.987
4	0.31	0.994
5	0.23	0.998
Ref	0.11	1.00

0.1 g/s (value corresponding to the 50 l/min in the entire tile) to 10 g/s. The (grid independent) results are shown in Fig. 3, with the expected quadratic dependence.

The Darcy-Forchheimer formulation in Eq [1].:

$$-\frac{dp}{dx} = P_v v_s + P_i v_s^2 \tag{1}$$

is adopted to describe the pressure drop in the equivalent porous medium, where p is the pressure, x is the spatial coordinate along the fluid flow direction, v_s is the seepage velocity (i.e., the apparent velocity through the bulk of the porous medium) and P_v and P_i are the viscous and inertia coefficients. Note that Eq [1]. does not require explicitly, at this stage, to set a value for the porosity, which would be an arbitrary number since the porous medium is here just a computational trick to reduce the computational effort of the numerical model. The values of P_v and P_i are derived best-fitting the computed values from the MC simulations, imposing the intercept at zero, resulting in a $R^2 = 1$, as shown in Fig. 3.

2.2. Thermal characteristic

For the thermal characterization of the porous strip, a simulation of the sub-domain geometry with the 6 MC in parallel as in Fig. 2a has been performed, imposing a uniform heat flux on the tungsten surface of 5 MW/m^2, which guarantees to keep the fluid in sub-cooled conditions everywhere (no local boiling), when the mass flow rate is kept to the nominal value of 0.5 g/s. Investigating more in detail the outcome of the CFD simulation, with the computed temperature map shown in Fig. 4a, one can easily evaluate few Key Performance Indicators (KPIs) such as the average, maximum and minimum temperature increase on the tungsten heated surface ($\Delta T_{ave,P0}$, $\Delta T_{max,P0}$ and $\Delta T_{min,P0}$, respectively), the average temperature increase of the interface surface between the tungsten and the copper ($\Delta T_{ave,\ P1}$), the average temperature increase of the copper facing the manifolds ($\Delta T_{ave,P2}$) and of the copper surface on back of the manifolds ($\Delta T_{ave,P3}$), (see Fig. 4).

Moreover, the thermal power entering the fluid directly from the tungsten layer (Q_H, in the horizontal direction) and indirectly from the copper layers within the MCs (Q_V, in the vertical direction), can be computed. The KPIs are reported in Table 2. Please note that the horizontal and vertical heat flows were obtained using summation of surface average reports on the 1 vertical face and 2 horizontal faces of each MC.

Similar behavior of the equivalent porous medium to the MC is obtained relying on the local thermal equilibrium (LTE) model, using the porosity as fitting parameter in the effective thermal conductivity k_{eff}^{iso} of the porous medium, first considered as an isotropic medium. It is known that, in the LTE model, a general definition of k_{eq} can be given using in Eq [2]:

$$k_{eff}^{iso} = \left(1-\varphi\right)k_{Cu} + \left(\varphi\right)k_{H2O} \tag{2}$$

where φ is the porosity, and k_{Cu} and k_{H2O} are the copper and water thermal conductivity, respectively. Eq [2]. allows fitting the thermal conductivity in the range 0.62 W/mK (the value of k_{H2O}) to 385 W/mK (the value of k_{Cu}) for a fitting value of the porosity changing from 1 to 0. The best fit value for k_{eff}^{iso} is obtained from the minimization of the error on the heated surface ε_{surf} in Eq. (3), and results in $k_{eff}^{iso} = 14.2$ W/mK,

$$\varepsilon_{surf} = \varepsilon\left(\Delta T_{max,W}\right) \times \varepsilon\left(\Delta T_{ave,W}\right) \times \varepsilon\left(\Delta T_{min,W}\right) \tag{3}$$

While the KPIs related to temperature increase show acceptable agreement between the PS and the MC simulations (see Table 2), the agreement on the split of the power entering the water channel in horizontal vs. vertical direction is poor. This fact is not surprising, since the heat transfer surface for the vertical heat flux in the MCs is 6 times larger than in the PS. The difference in the heat transfer surface can be counterbalanced if an anisotropic thermal conductivity k_{eq}^{aniso} is adopted. The vertical component $k_{eq,V}^{aniso}$ can be evaluated through Eqs [4–6].:

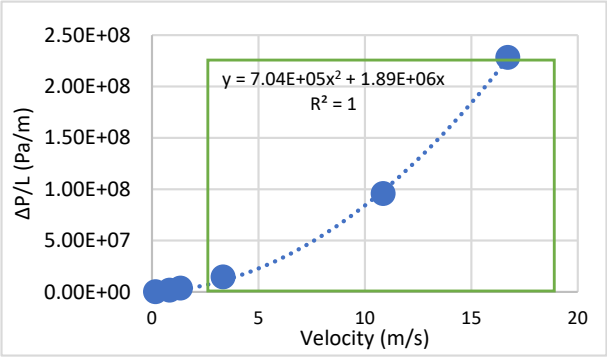

Fig. 3. Hydraulic characteristic (pressure gradient as a function of the average fluid velocity in the MCs) computed for the 6 MC connected in parallel (solid symbols), and quadratic fit according to Eq [1]. (marked area represents the turbulent fluid regime).

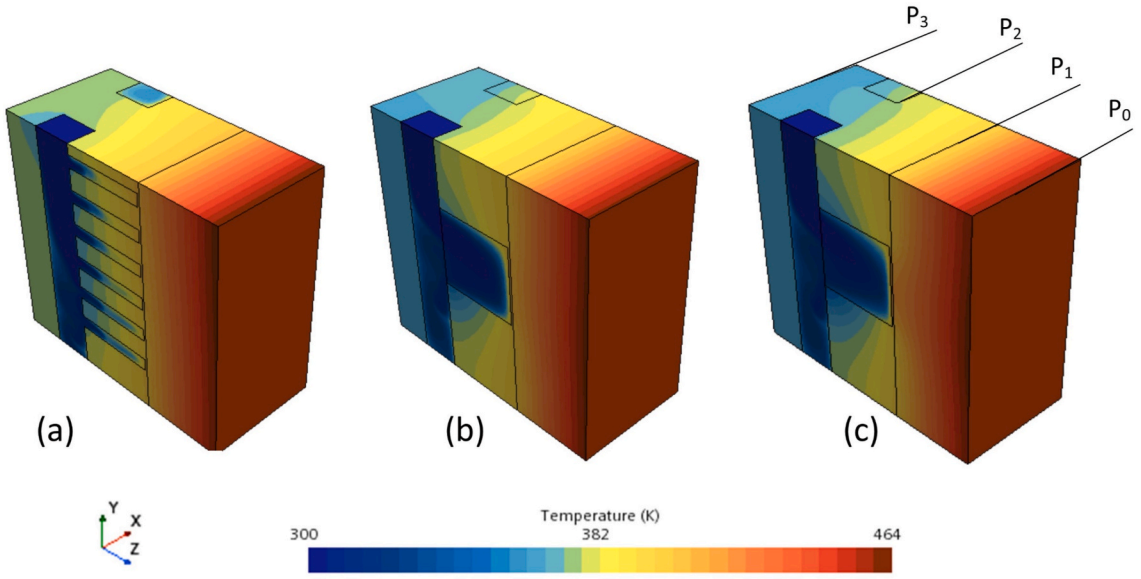

Fig. 4. Computed temperature map on (a) the simplified geometry with 6 MCs in parallel, (b) a porous strip with isotropic and (c) anisotropic thermal conductivity, respectively, for a surface load of 5 MW/m^2 and a cooling flow rate of 0.5 g/s. In (c), the x-y surfaces on which the KPIs are computed are also indicated.

Table 2
KPIs for the thermal-hydraulic simulations on the sub-size domain, for surface load of 5 MW/m^2 and a cooling flow rate of 0.5 g/s.

KPI	Micro-channels	Porous Strip	
		Isotropic k_{eff}	Anisotropic k_{eff}
Q_H (W)	1.9	14.05	5.04
Q_V (W)	56.3	39.56	55.88
$\Delta T_{max,W}$ (K)	164.48	163.41	164.48
$\Delta T_{ave,W}$ (K)	162.03	161.70	162.07
$\Delta T_{min,W}$ (K)	160.05	160.03	159.65
$\Delta T_{ave,int}$ (K)	100.75	100.43	100.80
$\Delta T_{ave,Cu}$ (K)	76.23	73.84	70.63
$\Delta T_{ave,back}$ (K)	72.81	65.25	64.48

$$Q_H = k_{eff,H}^{aniso} \times A_V \times \partial T/\partial h \tag{4}$$

$$Q_V = k_{eff,V}^{aniso} \times A_H \times \partial T/\partial v \tag{5}$$

In Eq. [4], $k_{eff,H}^{aniso}$ is the component of the anisotropic thermal conductivity in the x-y plane (the horizontal direction), A_V is the heat transfer surface for the horizontal heat flux (thus oriented in the vertical direction V) and $\partial T/\partial h$ is the temperature gradient in the horizontal direction. In Eq. [5], A_H is the heat transfer surface for the vertical heat flux (thus oriented in the horizontal direction H) and $\partial T/\partial v$ is the temperature gradient in the vertical direction. Assuming the two temperature gradients are comparable and sticking to the values of Q_H and Q_V resulting from the MC analysis in Table 2, the value of $k_{eff,V}^{aniso}$ can be computed as a function of $k_{eff,H}^{aniso}$ as reported in Eq [6]. The ratio between A_H and A_V is reduced to the ratio between the height and twice the value of the width of the PS, i.e. to 1.8 mm and 2×2 *mm*, respectively.

$$k_{eff,V}^{aniso} = 56.3\ W \Big/ 1.9\ W \times (1.8\ mm / 4\ mm) \times k_{eff,H}^{aniso}$$

$$\approx 13 \times k_{eff,H}^{aniso} \tag{6}$$

The best fit value for k_{eq}^{aniso}, computed again according to Eq. [4], returns the KPIs in Table 2, with a much better agreement on Q_V and Q_H with respect to the case with an isotropic value for the equivalent thermal conductivity of the porous medium.

A check of capability to reproduce the main features of the MC simulation with the PS model, calibrated as explained above, is performed checking the computed average temperature gradients with the coolant mass flow rate of 0.5 g/s in the three regions highlighted in Fig. 5. The maximum relative difference remains below 10%.

3. Validation of the porous strip model on a single array

The validation of the PS model is performed by analyzing an entire array (1 inlet and 1 outlet manifold, reduced to ½ to take advantage of the symmetry of the structure) with the detailed MC model and substituting the MCs grouped by 6 with the PS blocks, as shown by the geometry highlighted in Fig. 6. The simulation setup for this hybrid problem is analogous to that of the sub-domain used for the PS model calibration. Note the computational grid for the array equipped with 120 MC counts 21 MCells, while that with the PS is reduced to 2.1 MCells, with an obvious gain in the computational effort, as expected.

3.1. Flow and pressure distribution

A map of the pressure distribution along the manifolds for the array equipped with MC and with PS is shown in Fig. 6, and similar pressure levels are computed for both models for the given mass flow rate of 28 g/s. The lowest flow rate was chosen to analyse the heated configuration and check if the fluid remains in the single-phase region. The average computed pressure drop is reported as a function of the mass flow rate in Fig. 7a, where also the numerical uncertainty related to the grid selection is reported. The two hydraulic characteristics differ by few percent. As far as the flow repartition along the array and among the different MCs or PSs is concerned, the resulting distribution is reported in Fig. 7b and c, where the mass flow rate in the different PSs is compared to the sum of the mass flow rates in the MCs, grouped in groups of 6. The agreement is very good both qualitatively and quantitatively at all the different flow rates, either with and without the heat load applied on the tungsten surface, with a mean error of 9% in both cases. Note also that the tapering of the longitudinal manifolds is not sufficient to guarantee a uniform flow repartition all along the array.

3.2. Temperature distribution

As far as the thermal behavior is concerned, the verification of the PS model is done for a value of the inlet mass flow rate of 29 g/s, entering the array at 300 K and with a heat flux of 5 MW/m^2. The computed average temperature increase (with respect to the water inlet temperature) for the various porous strips and 6MCs along the array is shown in Fig. 8 both for the heated surface and for the tip of the fluid channels within the MC or PS. The average relative deviations from the results obtained with the detailed simulation of MCs are 11% for the heated surface. Note that the relative error increases significantly if we look at the average temperature on the tip of the porous strips, but mainly as an effect of the reduced flow rate in the PS #3–7, shown in Fig. 7c. To reduce the error of the temperature on the tip of the fluid, the thermal conductivity calibration could be re-done targeting the minimization of the error also of that aspect, but this is out of the scope of the present paper.

The heat penetration in the mock-up components around the hotspot region (with L = 0.02 m in Fig. 8a) shows that in the tungsten region the PS model predicts an overestimation on the temperature profile in the entire depth of the cover. As opposed to that, in the MC region, the cooling effect of the fluid is larger in the PS model than it is actually predicted by the MC model. In the solid casing made of copper, the PS model has still a slight overestimation of the temperature, which could be considered as a safety factor for engineering design purposes.

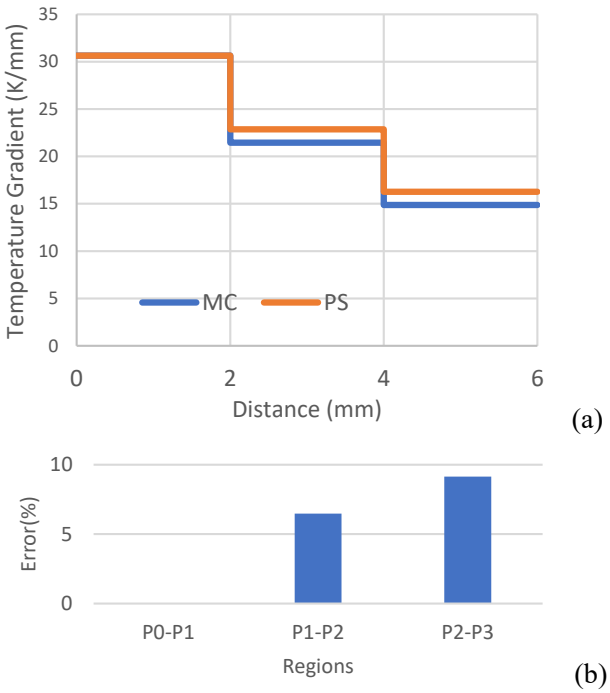

Fig. 5. (a) Average temperature gradient computed with the MC model and the PS model for of the mass flow rate of 0.5 g/s and (b) corresponding relative error of the PS model (see Fig. 4c for the locations of P_0 to P_3).

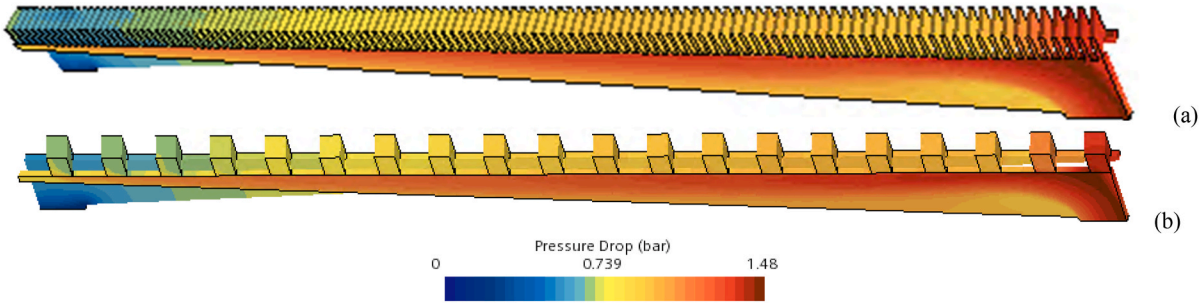

Fig. 6. Pressure map computed for the single array equipped with (a) MC and (b) PS for the inlet mass flow rate of 28 g/s.

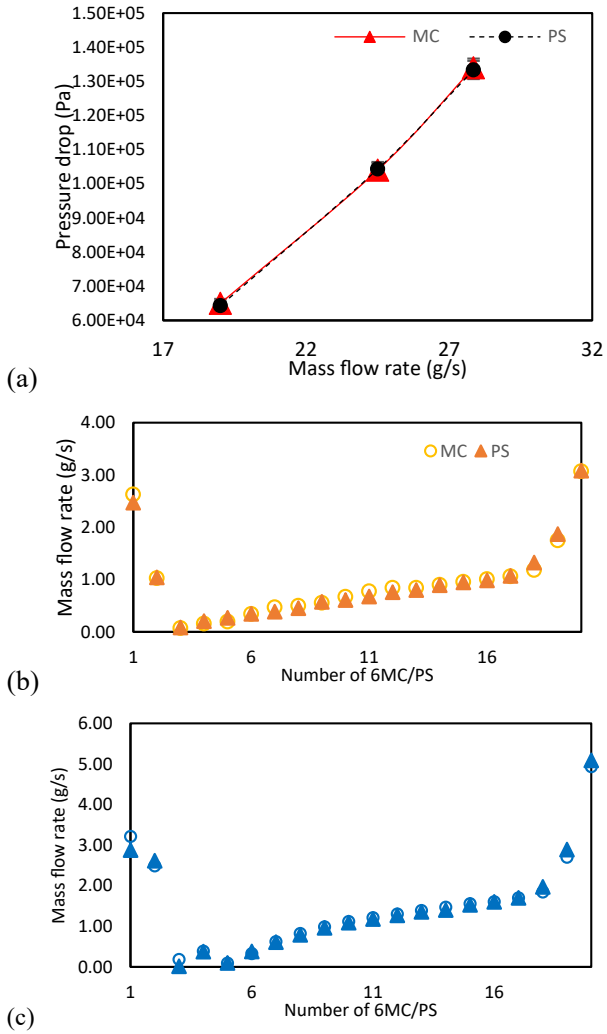

Fig. 7. Single array simulation results: (a) pressure drop computed with the MC and PS models, as a function of the flow rate, (b) mass flow rate repartition in the different PS and MC (grouped by 6) without and (c) with the applied heat load, for a total mass flow rate of 19 g/s.

4. Application to the whole divertor tile

The PS model has been applied to the entire 0.1 m × 0.1 m tile, substituting all the arrays equipped with MCs with the corresponding PS. Thanks to the symmetrical design of the divertor, the computational domain was reduced to half of the total geometry to ease the burden of computational costs. Therefore, the numerical grid for the entire half-tile counts 21.8 MCells. Fig. 9 shows the water

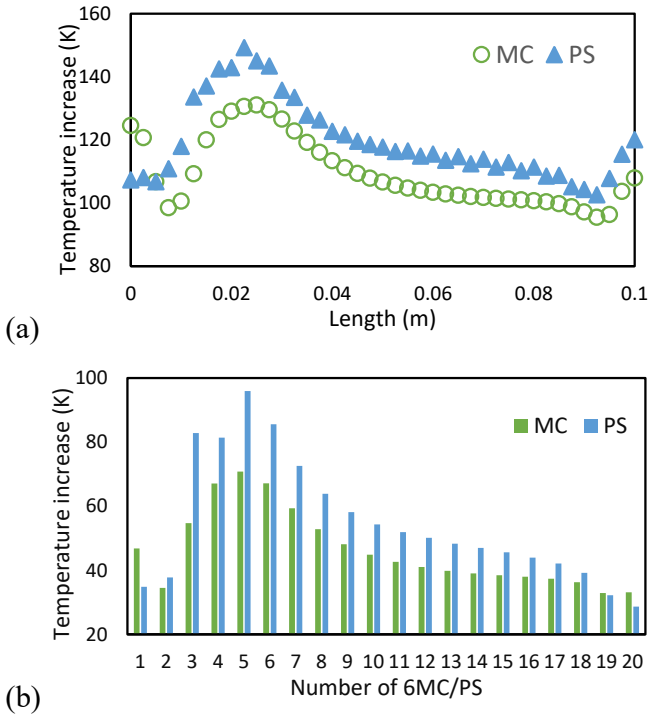

Fig. 8. Average temperature increase (a) on the heated surface, and (b) on the tip of the fluid channels computed in the simulation with MC and PS.

repartitioning among the manifolds. Please note that the value of the first manifold refers to the half manifold obtained after cutting the full geometry into two symmetrical halves. As shown, heating has some small effects on the flow rates, while the relationships between the manifolds remain constant. The tapering of the inlet and outlet manifolds allows reaching a pretty uniform flow repartition among the manifolds.

The pressure map on the fluid domain, as well as the temperature map on the heated surface, are reported in Fig. 10. The total computed pressure drop on the entire half-tile is 2.44 bar, while the temperature increase is ~15 K. The temperature map confirms that the location of the hotspots corresponds to what has been found in the array simulation, due to the minimum of the flow rate in the PSs, which leads a lower cooling effects. Note also the hot line at the edge of the tile, that is due to the presence of bulk material without cooling channels, as shown in Fig. 1.

5. Conclusions

In this study, a new hybrid approach was developed and used to model a divertor equipped with micro channels. In the first step and to reduce the burden of the MC modeling it was assumed that a group of MCs in hydraulic parallel can be replaced by a porous strip and the hydraulic and thermal characteristics of the new equivalent porous elements were determined and calibrated based on the reference MCs. Results showed that the proposed methodology is associated with an acceptable level of accuracy for hydraulic (9%) and thermal simulations (11% on the heated surface), when the PS model is compared with MC model in an array-scale. The obtained thermal and hydraulic characteristics were adopted in the simulation of the whole tile, computing for it a pressure drop of 2.4 bar for the flow rate of 50 l/min. According to the validation results on the single array, the computed hot spot of ~470 K on the tile edge should be a conservative value. The overall results, with a good expected accuracy on the computed local temperature gradients could be used to feed a thermo-mechanical model to evaluate the local stresses.

Author statement

Hossein Ebadi: Conceptualization, Methodology, Software, Formal analysis, Investigation, Validation, Data curation, Visualization, Writing - Review & Editing.

Francesco Carrone: Methodology, Software, Visualization, Writing - Review & Editing.

Rosa Difonzo: Conceptualization, Methodology, Software, Writing - Review & Editing.

Joris Fellinger: Methodology, Supervision, Writing - Review & Editing.

Heinrich P. Laqua: Supervision, Writing - Review & Editing.

Niko Schneider: Software, Writing - Review & Editing.

Laura Savoldi: Conceptualization, Methodology, Formal analysis, Investigation, Resources, Supervision, Writing - Original Draft.

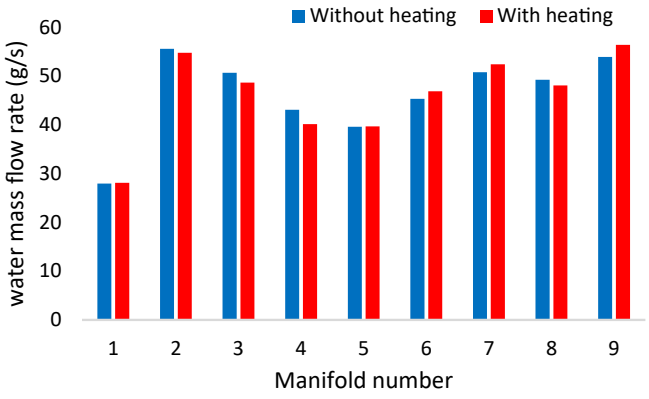

Fig. 9. Water repartitioning among the manifolds.

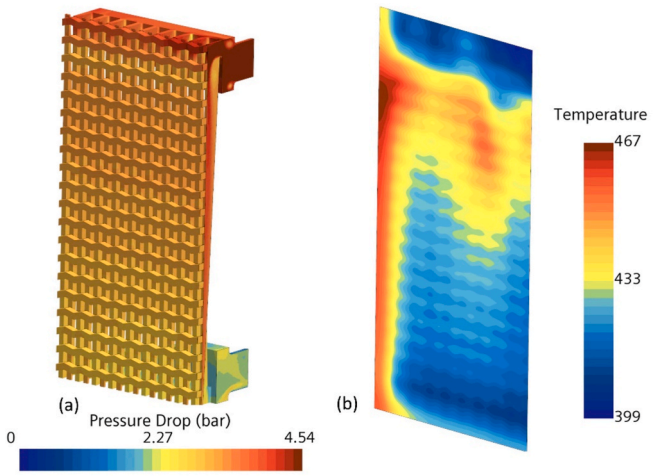

Fig. 10. Half tile equipped with PS, cooled with a flow rate of 0.4156 kg/s and subject to a uniform heat load of 5 MW/m^2: (a) computed pressure map and (b) computed temperature on the heated surface in K, for the inlet mass flow rate of 0.4156 kg/s.

Declaration of competing interest

The authors declare the following financial interests/personal relationships which may be considered as potential competing interests: Laura Savoldi reports financial support was provided by European Consortium for the Development of Fusion Energy.

Data availability

Data will be made available on request.

Acknowledgements

This work has been carried out within the framework of the EUROfusion Consortium, funded by the European Union via the Euratom Research and Training Programme (Grant Agreement No 101052200 — EUROfusion). Views and opinions expressed are however those of the author(s) only and do not necessarily reflect those of the European Union or the European Commission. Neither the European Union nor the European Commission can be held responsible for them.

References

[1] A. Horvath, E. Rachlew, Nuclear Power in the 21st Century: Challenges and Possibilities, Ambio, 2016.
[2] J. Adelerhof, M.B. Thoopal, D. Lee, C. Hardy, Clean and sustainable fusion energy for the future, PAM Rev. Energy Sci. Technol. 1 (2015) 20–42.
[3] J.L. Johnson, Stellarator and Heliotron Devices, Nucl Fusion, 1999.
[4] M. Wanner, J.H. Feist, H. Renner, J. Sapper, F. Schauer, H. Schneider, et al., Design and Construction of WENDELSTEIN 7-X, Fusion Eng Des, 2001.
[5] A. Iiyoshi, A. Komori, A. Ejiri, M. Emoto, H. Funaba, M. Goto, et al., Overview of the large helical device project, Nucl. Fusion 39 (1999) 1245–1256.

[6] T. Klinger, T. Andreeva, S. Bozhenkov, C. Brandt, R. Burhenn, B. Buttenschön, et al., Overview of first Wendelstein 7-X high-performance operation [Internet], Nucl. Fusion 59 (11) (2019 Jun 5), 112004 [cited 2022 Jun 20] Available from: https://iopscience-iop-org.ezproxy.biblio.polito.it/article/10.1088/1741-4326/ab03a7.
[7] H.-S. Bosch, Wendelstein 7-X upgrading for next experimental campaign [Internet]. [cited 2022 Sep 30]. Available from: https://www.euro-fusion.org/news/2021/june/wendelstein-7-x-upgrading-for-next-experimental-campaign-copy-1/.
[8] L. Li, L. Han, P. Zi, et al., Conceptual design and heat transfer performance of a flat-tile water-cooled divertor target [Internet], Plasma Sci. Technol. 23 (9) (2021 Jul 23) [cited 2022 Jun 21] Available from: https://iopscience.iop.org/article/10.1088/2058-6272/ac0689, 095601..
[9] J.H. Lim, M. Park, Flow boiling burnout in a hypervapotron channel under high heat flux and high sub-cooling conditions [Internet], J. Fusion Energy 41 (1) (2022 Jun 1) 1–12 [cited 2022 Jun 21] Available from: https://link.springer.com/article/10.1007/s10894-022-00316-w.
[10] J.H. Lim, M. Park, S.H. Park, Experimental study on CHF of one-side heated rectangular heat sink with regard to fusion divertor cooling, Therm. Sci. Eng. Prog. 30 (2022 May 1), 101261.
[11] J.H. Lim, M. Park, Studies on heat transfer coefficient of a circular tube with twisted tape insert for high heat flux cooling applications, IEEE Trans. Plasma Sci. 50 (2) (2022 Feb 1) 459–469.
[12] S. Kumar Rai, R. Sharma, M. Saifi, R. Tyagi, A. Professor, D. Singh, et al., Review of recent applications of micro channel in mems devices [Internet], Int. J. Appl. Eng. Res. 13 (9) (2018) 64–69 [cited 2022 Jun 22] Available from, http://www.ripublication.com.
[13] L. Savoldi, K.A. Avramidis, F. Albajar, S. Alberti, A. Leggieri, F. Sanchez, et al., A validation roadmap of multi-physics simulators of the resonator of MW-class CW gyrotrons for fusion applications, Energies 14 (2021) 8027 [Internet]. 2021 Dec 1 [cited 2022 Jan 6];14(23):8027. Available from: https://www.mdpi.com/1996-1073/14/23/8027/htm.
[14] H. Greuner, B. Boeswirth, J. Boscary, P. McNeely, High heat flux facility GLADIS:: operational characteristics and results of W7-X pre-series target tests, J. Nucl. Mater. (2007 Aug 1) 367–370 (SPEC. ISS.):1444–8.
[15] O.K. Siddiqui, M. Al-Zahrani, A. Al-Sarkhi, S.M. Zubair, Flow distribution in U- and Z-type manifolds: experimental and numerical investigation, Arabian J. Sci. Eng. 45 (7) (2020 Jul 1) 6005–6020 [cited 2022 Jun 22] Available from: https://link.springer.com/article/10.1007/s13369-020-04691-4.
[16] J.M. Hassan, T.A. Mohamed, W.S. Mohammed, W.H. Alawee, Modeling the uniformity of manifold with various configurations, J Fluids (2014) 1–8, 2014 Aug 24.
[17] L. Savoldi, A. Allio, P. Arena, A. Del Nevo, Hybrid modelling for the manifolds and coolant flow distribution in the Water-Cooled Lead-Lithium of the EU-DEMO reactor, in: Proceedings of the 19th International Topical Meeting on Nuclear Reactor Thermal Hydraulics (NURETH-19), 2022.
[18] D. Rehman, G.L. Morini, Experimental validation of a two equation RANS transitional turbulence model for compressible microflows, Int. J. Heat Fluid Flow 86 (2020 Dec 1), 108711.
[19] Siemens PLM Software Inc, Star-CCM+ User's Guide V. 15.02, Plano, TX, USA, 2020.